

Note : For shorter optical cycles or more weakly bound (slow) electrons, the adiabatic ADK model eventually breaks down.

Lecture 3

A.3 Strong c.w fields

- S matrix theories (non adiabatic in $\vec{E}(t)$!)

recall 1. order PT (page 3)

$$P_{a \rightarrow \vec{p}}(t) = \left| \int_{-\infty}^t dt' \langle \vec{p} | H_{int}(t') | a \rangle e^{i\omega_a t} \right|^2$$

1. order in $I \sim |E|^2$

KFR theory

$$\langle \vec{r} | \vec{p} \rangle e^{-i\omega_{\vec{p}} t} = (2\pi)^{3/2} \exp \left\{ i\vec{p} \cdot \vec{r} - \frac{1}{2} \int_{-\infty}^t dt' (\vec{p} + \vec{A}(t'))^2 \right\}$$

"Volkov final state": all orders in I !

⇒ num. differential ionization probs. for n-photon ionization

$$dP_{a \rightarrow \vec{p}} = 4\pi^2 \left| \frac{I_p + p^2/2}{\omega} \right| J_n \left(\frac{\vec{E}_0 \cdot \vec{p}}{\omega^2}, \frac{U_p}{2\omega} \right) \tilde{\varphi}_a(\vec{p})^2 d\vec{p}$$

I_p : ioniz. potential

$U_p = \frac{E_0^2}{4\omega^2}$: ponderomotive energy

$J_n(x, y) = \sum_{j=-\infty}^{\infty} J_{n+2j}(x) J_j(y)$: gen. Bessel fact

$\tilde{\varphi}_a(\vec{p}) = (2\pi)^{-3/2} \int d\vec{r} \varphi_a(\vec{r}) e^{i\vec{p} \cdot \vec{r}}$: initial state

cf. H. R. Reiss, Phys. Rev. A 22, 1786 (1980) and refs to Faisal & Keldysh papers therein.

PPT theory

Add Coulomb interaction to laser interaction

≡ Coulomb-Volkov final state

⇒ analytical expression for ionization rate $T_{PPT}^I(E_0)$

- cf. Perelomov, Popov, Terent'ev, Sov. Phys. JETP 23, 924 (1966) (15)
 Popruzhenko & D. Bauer, J. Mod. Opt. 55, 2573 (2008)
 C.-H. Zhang & U. Thumm, Phys. Rev. A 82, 043405 (2010)

- Floquet Ansatz for monochromatic fields

Laser-matter interaction

$$H_{\text{int}}(t) = H_{\text{int}}(t+T), \quad T = \frac{2\pi}{\omega}$$

e.g. : $H_{\text{int}} = -i \vec{A} \cdot \vec{\nabla}, \quad \vec{A}(t) = \vec{A}_0 \cos \omega t$

periodicity implies discrete Fourier expansion

$$H_{\text{int}}(t) = \sum_{n=-\infty}^{\infty} H_{\text{int}}^{(n)} e^{-in\omega t} \quad (*)$$

TDSE

$$\underbrace{(H_0 + H_{\text{int}}(t))}_{H(t)} \psi(t) = i \frac{\partial}{\partial t} \psi \quad (**)$$

periodicity motivates Ansatz

$$\psi(t) = e^{-iEt} \underbrace{\sum_{n=-\infty}^{\infty} F_n e^{-in\omega t}}_{=: \mu_E(t)}$$

note:

energy = $E + n\omega$

"Quasi energies" E : cast TDSE in TISE form

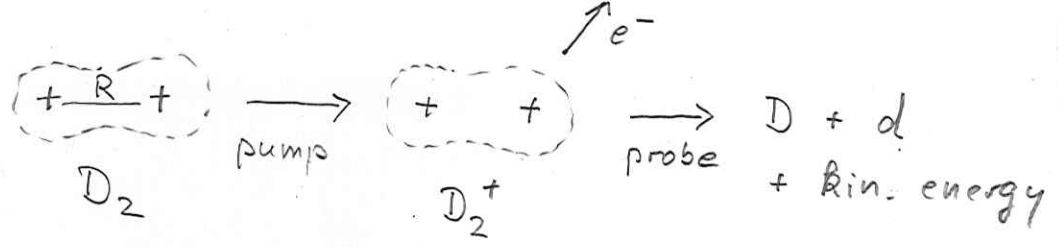
$$H \psi = i \frac{\partial}{\partial t} \psi \Leftrightarrow (H - i \frac{\partial}{\partial t}) \mu_E = E \mu_E$$

(**) \Leftrightarrow system of time-independent coupled equations:

$[E + n\omega - H_0] F_n(\xi) = \sum_{R=-\infty}^{\infty} H_{\text{int}}^{(n-R)} F_R(\xi)$	all spatial coordinates \uparrow
$\text{or } [H_{\text{Floquet}} - E] \vec{F}(\xi) = 0$	

\uparrow matrix \uparrow $\begin{pmatrix} F_{-\infty} \\ \vdots \\ F_0 \end{pmatrix}$

(cf. extra sheet)



Floquet picture:

Application to identify light-induced molecular dissociation pathways

PHYSICAL REVIEW A 79, 033410 (2009)

Quantum-beat imaging of the nuclear dynamics in D_2^+ : Dependence of bond softening and bond hardening on laser intensity, wavelength, and pulse duration

Maia Magrakvelidze,¹ Feng He,¹ Thomas Niederhausen,²
Igor V. Litvinyuk,¹ and Uwe Thumm¹

¹James R. Macdonald Laboratory, Kansas State University, Manhattan, Kansas 66506-2604, USA
²Departamento de Química, C-IX, Universidad Autónoma de Madrid, 28049 Madrid, Spain

(Received 30 January 2009; published 18 March 2009)

Based on a quantum-mechanical model, we calculate the time evolution of an initial nuclear vibrational wave packet in D_2^+ generated by the rapid ionization of D_2 in an ultrashort pump-laser pulse. By Fourier transformation of the nuclear probability density with respect to the time delay between the pump pulse and the instant destructive Coulomb-explosion imaging of the wave packet at the high-intensity spike of an intense probe-laser pulse, we provide two-dimensional internuclear-distance-dependent power spectra that serve as a tool for visualizing and analyzing the nuclear dynamics in D_2^+ in an intermittent external laser field. The external field models the pedestal to the central ultrashort spike of a realistic probe pulse. Variation in the intensity, wavelength, and duration of this probe-pulse pedestal (i) allows us to identify the optimal laser parameters for the observation of field-induced bond softening and bond hardening in D_2^+ and (ii) suggests a scheme for quantitatively testing the validity of the "Floquet picture" that is commonly used for the interpretation of short-pulse laser-molecule interactions, despite its implicit "continuum wave" (infinite pulse length) assumption.

Fragmentation mechanisms

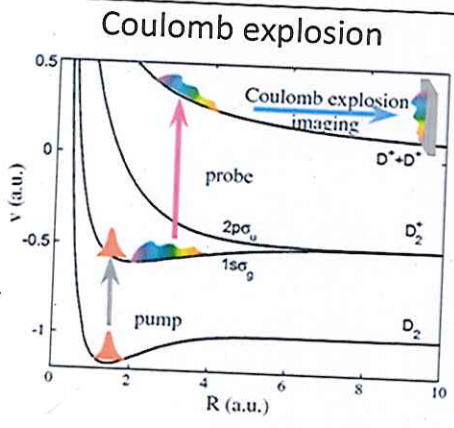


FIG. 1. (Color online) Schematic of the simulated KER measurement underlying the frequency-resolved investigation of the nuclear dynamics in D_2^+ discussed in this work. The pump-laser pulse launches a nuclear wave packet onto the D_2^+ $1s\sigma_g^+$ potential curve by ionizing D_2 and starts the molecular clock. After an adjustable time delay, an intense short probe pulse promotes the nuclear wave packet onto the $2D^+$ repulsive $1/R$ Coulomb-explosion curve and allows for the detection of the fragment-kinetic-energy distribution.

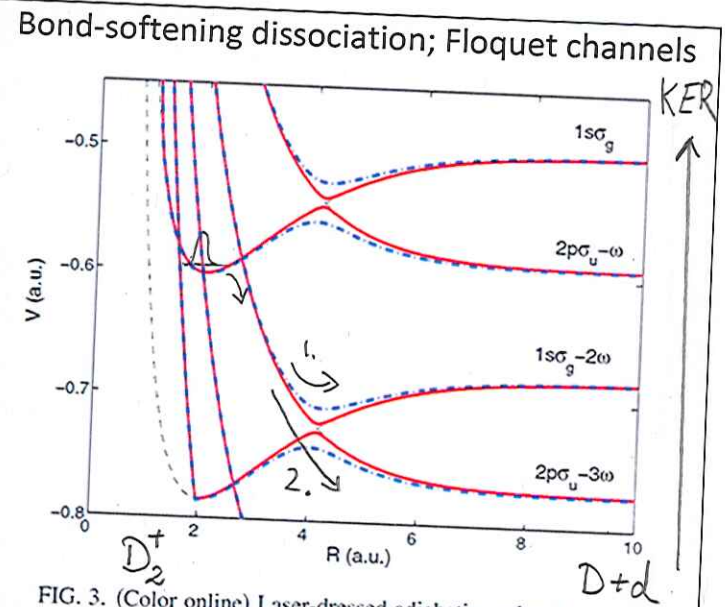


FIG. 3. (Color online) Laser-dressed adiabatic molecular potential curves for D_2^+ and a 500 nm cw laser field with an intensity of 5×10^{11} (solid red lines) and 10^{13} W/cm² (dashed-dotted blue lines). Thin black dashed lines show field-free BO potential curves.

KER : fragment kinetic energy release

All of this is gauge independent - so far.

In the length or velocity gauge:

$$H_{int} = H_+ e^{-i\omega t} + H_- e^{i\omega t}$$

⇒ in (*) on p. 15 only two frequencies ($\pm\omega$) contribute

$$\Rightarrow [\mathcal{E} + n\omega - H_0] F_n = H_+ F_{n+1} + H_- F_{n-1}$$

i.e. $H_{Floquet}$ is tri-diagonal

cf. G. Floquet, Ann. Ec. Norm (2) 13, 47 (1883)
S. I. Chu, Adv. At. Mol. Phys. 21, 197 (1985)

Application to multi-photon ionization

$$\mathcal{E} = \mathcal{E}_0 + \Delta - i\Gamma/2$$

↑ AC Stark shift

unperturbed (field-free) initial state energy

Γ : ionization rate ("total": i.e. for all electrons)

Gauges

So far, we discussed examples in the velocity gauge:

$$[H_0 + \vec{A}(t) \cdot \vec{P}] \psi_{VG} = i \frac{\partial}{\partial t} \psi_{VG}$$

↑
mom. operator

A unitary transformation connects to the length gauge:

$$\psi_{LG} = e^{i\vec{A} \cdot \vec{r}} \psi_{VG}; \quad \partial_{LG} = e^{i\vec{A} \cdot \vec{r}} \partial_{VG} e^{-i\vec{A} \cdot \vec{r}}$$

↑
for one e^- , otherwise = \sum coord. vectors

$$[H_0 + \vec{E}(t) \cdot \vec{r}] \psi_{LG} = i \frac{\partial}{\partial t} \psi_{LG}$$

$$\vec{E}(t) = -\frac{1}{c} \frac{\partial \vec{A}}{\partial t}$$

cf YC Han + L B. Madsen, Phys. Rev. A 81, 063430 (2010):

Comparison of HAG spectra calculated in LG & VG

- Note:
- QM is gauge invariant
 - approximations may induce gauge variance
 - the numerical effort can be strongly gauge dependent

The gauge transformation

$$\psi_{VG} = e^{i \vec{\alpha}(t) \cdot \vec{P}} \psi_{AG} \quad (*)$$

$$\vec{\alpha}(t) := \int dt' \vec{A}(t') \quad (\text{displacement vector})$$

leads to the acceleration gauge ("Kramers - Henneberger" gauge):

For N electrons

$$\underbrace{\left[\sum_{i=1}^N \frac{P_i^2}{2} + V_{\text{atom}}(\vec{r}_1 + \vec{\alpha}, \dots, \vec{r}_N + \vec{\alpha}) \right]}_{H_0} \psi_{AG} = i \frac{\partial}{\partial t} \psi_{AG}$$

Interpretation:

- \vec{P} in (*) generates spatial translations by $\vec{\alpha}(t)$
- This corresponds to a transformation from the lab. frame to a non-inertial frame, in which all electrons "see" an oscillating nucleus.
- The influence of \vec{E} is completely contained in this oscillation.
- For linear polarization:

$$\vec{E}(t) = E_0 \hat{E} \cos \omega t$$

$$\vec{\alpha}(t) = \alpha_0 \hat{E} \cos \omega t$$

$$\alpha_0 = \frac{E_0}{\omega^2} \quad \text{"excursion amplitude"}$$

\approx excursion range in class. rescattering model

High-frequency Floquet theory

acceleration gauge, expand in Fourier series

$$V(\vec{r} + \vec{x}(t)) = \sum_{n=-\infty}^{\infty} V_n(\vec{x}_0, \vec{r}) e^{-in\omega t}$$

$$\Rightarrow \left[\epsilon + n\omega - \frac{p^2}{2} - V_0(\vec{x}_0, \vec{r}) \right] F_n(\vec{r}) = \sum_{R \neq 0} V_{n-R}(\vec{x}_0, \vec{r}) F_R(\vec{r})$$

$V_0 \hat{=}$ static (time-averaged) "dressed" potential:

At high frequencies & high intensities, the atomic structure in the ext. (laser) field is essentially governed by V_0 .

Example: Pont et al., Phys. Rev. Lett 61, 939 (1988)

For $x_0 = 20$ a.u. these calculations show that V_0

- splits prob. density in two disjoint parts with maxima near classical excursion range $\pm x_0$.
- induces radiative stretching along light polarization (cf. extra sheet)

Adiabatic ionization stabilization

At sufficiently large light intensities I

ionization starts to decrease with increasing I .

Reason: the photoelectron's excursion range becomes large & inhibits ionization

Examples: Exp: Ne (5g) photoionization : de Boer et al

Theory: H (1s) - " - Dörr et al.

(cf. extra sheet)

Adiabatic stabilization against photoionization: An experimental study

M. P. de Boer, J. H. Hoogenraad, R. B. Vrijen, R. C. Constantinescu, L. D. Noordam, and H. G. Muller
Phys. Rev. A 50, 4085 (1994):

Experiment demonstrating light-induced stabilization against photoionization. For a 100-fs, 620-nm probe pulse, the optimum choice is the circular 5g state in neon. A picosecond pump laser was used to prepare this Rydberg state. When the probe intensity is several times 10^{13} W/cm² a decrease in yield with respect to a less intense pulse is observed, in accordance with theory.

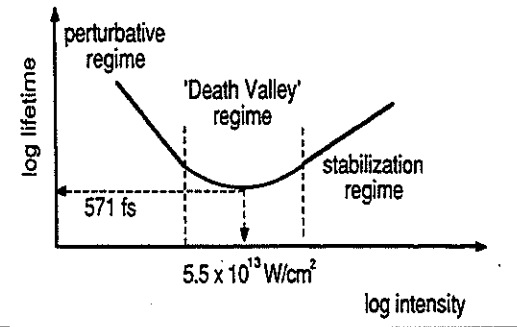
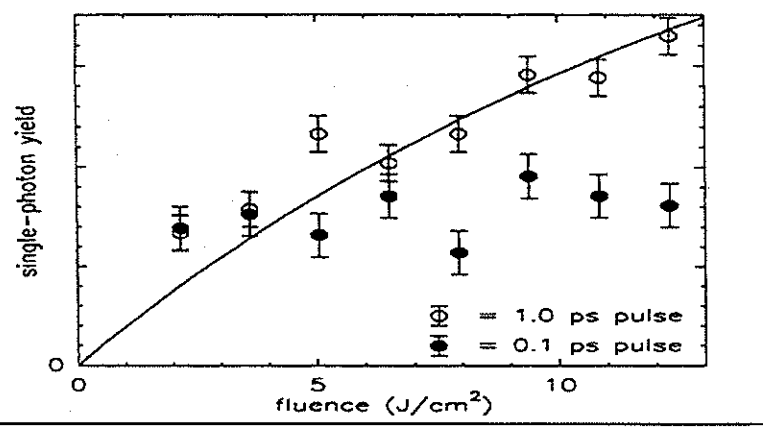
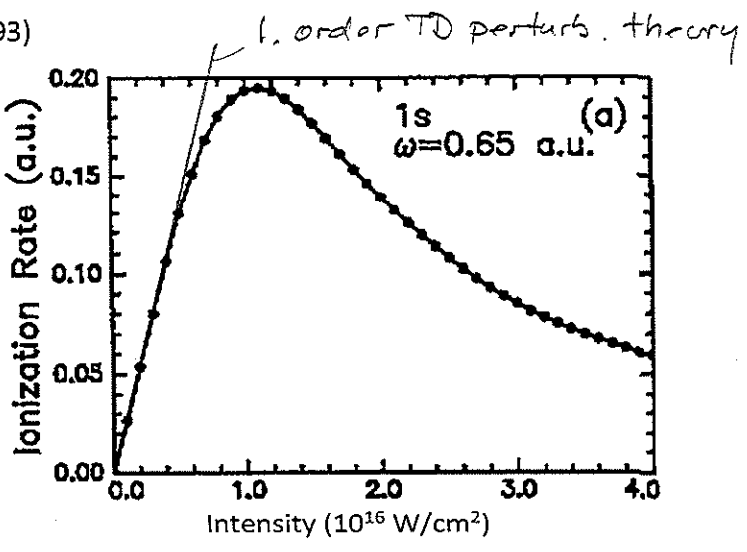


FIG. 12. Photoionization yield of the circular 5g state as a function of fluence. The open circles were measured with low peak intensity (up to 1.2×10^{13} W/cm², 1 ps). The curve represents a fit using the perturbative rate (including depletion) and an adjustable asymptotic value. The solid circles were measured using shorter pulses, with the same fluence but more intense (up to 12×10^{13} W/cm², 0.1 ps). The yield due to these pulses hardly increases with fluence, which indicates stabilization.

R-matrix-Floquet theory of multiphoton processes. III. Multiphoton ionization of atomic hydrogen

M Dorr¹, P G Burke¹, C J Joachain¹, C J Noble¹, J Purvis¹ and M Terao-Dunseath¹
J. Phys. B: At. Mol. Opt. Phys. 26 L275 (1993)

Using R-matrix-Floquet theory the authors have analysed the multiphoton ionization of atomic hydrogen from the ground and metastable 2s state in an intense, linearly polarized, monochromatic laser field. The authors discuss the limits of lowest order perturbation theory and find high-frequency stabilization at high intensities.



Note :

- linear increase of ionization rate T with I at low I (as predicted by lowest-order perturbation theory.)
- max. T at $\approx 10^{16} \text{ W/cm}^2$, then stabilization as $I \nearrow$ (Dör 1993).
- stabilization hard to reach in practise, since ionization likely on leading (and trailing) edge of light pulse ("death valley").
 \Rightarrow need short pulses to observe stabilization.

But :

Pulse raise time also needs to be long enough so that atom remains adiabatically in initial (ground) state.
 (Comparison of Floquet with time-dept. calculations show that both requirements can be met.)

- at shorter pulse-raise times, excited states of Kramers-Henneberger-gauge potential $V_0(\vec{x}_0, \vec{r})$ are populated and stabilization persists.
- trick: prepare atom in circular Rydberg state \Rightarrow stabilization at relatively low I (see extra sheet, de Boer expt., in fair agreement with theory: Dereaux & Potvliege, Phys. Rev. A 57, 5009 (1998)).

Dynamic stabilization

Different mechanism that relies on interference of electron wave packets (partial waves).

Works typically for $I \gtrsim 10^{14} \text{ W/cm}^2$.

E.g.: negative interference of resonance states with comparable widths

cf. Tikhonova, Fedorov, Laser Physics 7, 574 (1997).

B. Two electron atoms